A Rac-Pak signaling pathway is essential for ErbB2-mediated transformation of human breast epithelial cancer cells

Luis E. Arias-Romero[1], **Olga Villamar-Cruz**[1], **Almudena Pacheco**[1], **Rachelle Kosoff**[2], **Min Huang**[1], **Senthil K. Muthuswamy**[3], and **Jonathan Chernoff**[1,4]

[1] Fox Chase Cancer Center, 333 Cottman Ave, Philadelphia, PA 19111, USA

[2] Cancer Biology Program, University of Pennsylvania, Philadelphia, PA 19104, USA

[3] Ontario Cancer Institute, University of Toronto, Toronto, Ontario, Canada

Abstract

The activation of receptor tyrosine kinases, particularly ErbB2, plays an important role in the genesis of breast cancer. ErbB2 kinase activity promotes Ras-mediated stimulation of downstream protein kinase cascades, including the Ras/Raf-1/Mek/extracellular-signal regulated kinase (Erk) pathway, leading to tumor cell growth and migration. Signaling through the Ras-Erk pathway can be influenced by p21-activated kinase-1 (Pak1), an effector of the Rho family GTPases Rac and Cdc42. In this study, we asked if ErbB2 expression correlates with Pak1 and Erk activity in human breast cancer specimens, and if Pak1 signaling is required for ErbB2 transformation in a 3D *in vitro* setting and in xenografts. We found a correlation between ErbB2 expression and activation of Pak in estrogen-receptor positive human breast tumor samples and observed that in 3D cultures, activation of Rac-Pak1 pathway by ErbB2 homodimers induced growth factor independent proliferation and promoted disruption of three-dimensional mammary acinar-like structures through activation of the Erk and Akt pathways. Further, we found that inhibition of Pak1 by small molecules compromised activation of Erk and Akt, resulting in reversion of the malignant phenotype and restoration of normal acinar architecture. Finally, ErbB2-amplified breast cancer cells expressing a specific Pak inhibitor showed delayed tumor formation and down-regulation of Erk and Akt signaling *in vivo*. These data imply that the Rac-Pak pathway is vital to ErbB2-mediated transformation and that Pak inhibitors represent plausible drug targets in breast cancers in which ErbB2 signaling is activated.

Keywords

transformation; small GTPase; protein kinase; ErbB2; signal transduction; breast cancer

[4]corresponding author: Jonathan.Chernoff@fccc.edu, tel: 215 728 5319, fax: 215 728 3616.

Introduction

The human ErbB/Her receptor family comprises four tyrosine kinase receptors (HER1/ ErbB1, also termed the epidermal growth factor receptor (EGFR), HER2/ErbB2, HER3/ ErbB3, and HER4/ErbB4) that play important roles in the progression of various types of cancers, including breast, prostate, and colon cancer. Deregulation of ErbB receptor signaling leads to enhanced cell proliferation, migration, and malignant transformation (Hynes & MacDonald, 2009). Overexpression, amplification, or mutation of the *ERBB2* gene occurs in about 25% of human breast cancer, and is associated with disease progression, metastasis, and poor prognosis, and a blocking antibody for ErbB2 is widely used for breast cancer therapy (Shalaby *et al.*, 1992a; Shalaby *et al.*, 1992b). However, the cellular and molecular mechanisms by which ErbB2 enhances the growth and survival of cancer cells are not completely understood. It is known that ErbB2 kinase activity promotes Ras-mediated stimulation of the Raf/MEK/Erk and Akt pathways leading to tumor cell growth, migration, and enhanced survival (Amundadottir & Leder, 1998; Karunagaran et al., 1996). Several reports suggest that signaling through the Ras-Erk and Akt pathways can be influenced by p21-activated kinase 1 (Pak1), an effector of the Rho family GTPases Rac and Cdc42 (Beeser *et al.*, 2005; Eblen *et al.*, 2002; Higuchi *et al.*, 2008; Mao *et al.*, 2008). Since Paks are central nodes for multiple signaling pathways (Arias-Romero and Chernoff, 2008; Bokoch, 2003; Jaffer and Chernoff, 2002), over-expression of these kinases in tumor cells could potentially alter cytoskeletal remodeling, cell survival and growth. An increase in the Rac and Pak protein levels has been observed in several human tumors (Dummler et al., 2009; Schnelzer et al., 2000). In human breast cancer tumors, a correlation between high grade, protein level, and the kinase activity of Pak1 has been reported (Holm et al., 2006). Recently, Li et al. showed that the inhibition of Pak1 activity in a series of Ras-transformed MCF-10A three-dimensional (3D) cultures, reduced proliferation, migration/invasion, and proteolysis, and also promoted luminal clearing in developing acini (Li et al., 2008). However, the mechanism(s) by which Pak regulates these cellular events, and their relevance to ErbB2 signaling, are not clear.

In this paper, we sought to clarify the molecular mechanism(s) by which the Rac-Pak pathway contributes to ErbB2 signaling in breast epithelial cells. Using a breast cancer tissue microarray, we observed a significant correlation between the expression levels of ErbB2 and the phosphorylation levels of Pak. Additionally, we used a 3D *in vitro* model to recapitulate the architectural elements of breast acinar development, while retaining the ability to manipulate and analyze the pathways that underlie the effects of Rac and Pak on ErbB2 signaling. Consistent with its proposed role in oncogenic signaling, we found that activation of ErbB2 promotes the activation of Rac and Pak, and that inhibition of Rac and Pak activity by expressing dominant negatives forms of Rac1 or Pak1, or by using small molecule inhibitors, impeded the ability of activated ErbB2 to transform these cells and to activate Erk and Akt. In addition, we found that the over-expression of constitutively activated Rac and Pak in breast epithelial cells distorted normal acinar morphology, causing unchecked proliferation, and loss of polarity. These effects were associated with Erk and Akt activation and required the kinase activity of Pak. Finally, we observed that MDA-MB-361/DYT2 cells expressing PID formed significantly smaller tumors than cells

expressing either GFP or the inactive PID in SCID mice as the result of the inhibition of Erk and Akt signaling. These results support a model in which Pak, by activating the Raf/Mek/Erk and Akt pathways, cooperates with ErbB2 in transforming mammary epithelial cells.

Results

Overexpression of ErbB2 correlates with activation of Pak

The tissue microarrays containing normal and tumor samples were stained for ErbB2 (Fig. 1A). We observed that this RTK was expressed in 73 of 209 (34.8%) breast tumors investigated. To examine whether ErbB2 expression is correlated with the activation of Pak, we performed an immunohistochemical staining for phospho-Pak (Fig. 1A). Overall, we found a weak correlation between ErbB2 expression and the levels of active Pak (rho = 0.2938, p<0.0001) (Fig. 1B). However, when the samples were stratified according to estrogen receptor (ER) status, we found a strong correlation between ErbB2 and phospho-Pak in ER-negative tumors (rho = 0.433, p<0.0001), but no correlation in ER-positive samples (rho −0.0428) (Fig. 1C). These results suggest that ErbB2 may modulate Pak signaling in ER-negative mammary tumors.

Pak is required for ErbB2-mediated transformation of MCF-10A cells

To establish the functions of group I Paks in human breast epithelial cells, we examined the effects of these kinases in ErbB2 signaling in MCF-10A cells grown in 3D conditions. MCF-10A cells are immortalized, non-transformed cells derived from a reduction mammoplasty, that form organized acini when grown within 3D matrices such as reconstituted basement membrane (rBM) (Muthuswamy et al., 2001; Soule et al., 1990). In MCF-10A cells that stably express an AP1510-activatable, chimeric form of ErbB2 (10A.ErbB2 cells), treatment with AP1510 caused characteristic changes in acinar morphogenesis, luminal apoptosis, and proliferation, resembling those seen in human ductal carcinoma of the breast (Muthuswamy et al., 2001) (Fig. 2A). We found that activation of ErbB2, promotes activation of Rac and Pak, consistent with the documented activation of these signaling proteins by other receptor protein tyrosine kinases (Supplementary Fig. 1A) (Beeser *et al.*, 2005; Frost *et al.*, 1997; Menard and Mattingly, 2003).

Next, we asked if Pak activity is required for the phenotypic effects of ErbB2 on acinar development. We used Tet-Off recombinant adenoviruses encoding dominant negative (DN) forms of Rac1 and Pak1, or a Pak inhibitory peptide (PID) to block Pak activity in 10A.ErbB2 cells. These viruses allowed tightly regulated expression of the transgenes (Supplementary Fig. 1B). Data were quantitated by analyzing immunofluorescence images from confocal image slices through the entire acinus (Supplementary Fig. 2). Transduction of 10A.ErbB2 cells with recombinant adenoviruses encoding DN Rac1, DN Pak1, or the PID had little effect on basal rates of cell proliferation or apoptosis, nor did they affect acinar architecture; however, the phenotypic effects of ErbB2 activation were blocked in cells expressing these dominant negative mutants (Fig. 2A and Supplementary Fig. 3A).

To ensure that these effects were due to loss of Pak activity, we carried out similar experiments using two different, highly specific small molecule inhibitors of Rac1 and group I Paks, NSC23766 (Gao et al., 2004) and IPA-3 (Deacon et al., 2008), respectively. As with the DN mutants, chemical inhibition of Rac-Pak pathway suppressed the multi-acinar effects of ErbB2, and these cells displayed normal rates of cell proliferation or apoptosis (Fig. 2B). Together, these data show that Rac-Pak function is required by ErbB2 to induce a multiacinar phenotype.

In human breast cancer cells, ErbB2 usually heterodimerizes with ErbB1 to propagate signals. Since activation of 10A.ErbB2 cells with the crosslinker AP1510 induces an ErbB2:ErbB2 homodimer, we also tested the effects of inhibiting Rac or Pak in 10A.ErbB2/ ErbB1 cells, which are engineered to form an ErbB2:ErbB1 heterodimer upon addition of the crosslinker AP21967 (Zhan et al., 2006). In this system, we found that small molecule inhibitors of either Rac or Pak reversed the effects of ErbB2:ErbB1 signaling (Fig. 2C). Thus, in both ErbB2 model cell lines cultured in 3D settings, blockade of Rac or Pak has significant effects on ErbB2-generated oncogenic signals.

Activated Pak bypasses requirement of ErbB2 activity for transformation

Treatment of 10A.ErbB2 cells with the Rac and Pak inhibitors blocked the effects of ErbB2 activation on acinar morphology (Figs. 2B, 2C). If Pak activation downstream of ErbB2 and Rac mediates the effects of ErbB2 on signal transduction, then constitutively active (CA) forms of Rac and Pak should bypass the need for ErbB2 in signaling. We transduced 10A.ErbB2 cells with Tet-Off recombinant adenoviruses encoding CA Rac1 or CA Pak1, plus an adenovirus encoding a tetracycline transactivator (Supplementary Fig. 1B). Cells expressing these activated mutants displayed aberrant acini, high rates of cell proliferation, and suppression of apoptosis even in the absence of activated ErbB2 (Fig. 3, and Supplementary Fig. 2 and 3B).

Molecular Pathways affected by Pak in MCF-10A cells

We next tested if Pak links ErbB2 to Erk in MCF-10A cells. First, we assessed ERK activity in response to ErbB2. 3D cultures of 10A.ErbB2 cells were treated with AP1510 and Erk activity assessed by immunoblot using phospho-specific antibodies. As expected, activation of ErbB2 induced activation of Erk (Fig. 4A). In contrast, in cells expressing DN forms of Rac1 or Pak1, or the PID or treated with small molecule inhibitors of Rac1 and Pak, Erk activation by ErbB2 was markedly suppressed (Fig. 4A). It should be noted that the Pak inhibitor IPA-3 has no significant inhibitory activity against recombinant Mek *in vitro* (Deacon et al., 2008). In contrast, in cells expressing active forms of Rac1 or Pak1, Erk activity was elevated even in the absence of activated ErbB2 (Supplementary Fig. 4A). Similar results were seen regarding two other important signaling molecules that are activated by Pak, namely Akt and BAD (Fig. 4B, 4C, and Supplementary Fig. 4B, 4C). Importantly, the effects of Pak on ErbB2 signaling were not confined to 10A.ErbB2 cells. As in 10A.ErbB2 cells, addition of specific Rac and Pak inhibitors to theErbB2-expressing human breast cancer cell lines MDA-MB-631, BT-474, BT-20, and SKBR-3, and resulted in appreciable loss of ERK activity (Supplementary Fig. 5). Finally, inhibition of Erk signaling

by the small molecule inhibitor PD 98059 restored normal acinar morphology (Supplementary Fig. 6).

Down regulation of Pak inhibits the tumorigenicity of ErbB2 positive breast cancer cells *in vivo*

To define the role of Pak in the proliferation of ErbB2-expressing human breast cancer cells, we generated MDA-MB-631/DYT2 stable cell lines that express GFP, GFP-PID or the inactive GFP-PID L107F. As in 10A.ErbB2 cells, blockade of Pak by PID expression suppressed cell proliferation and activation of Erk in MDA-MB-631/DYT2 cells (Fig. 5A and 5B). To determine a role of Pak in tumor formation, we injected these three cell lines into the flanks of SCID mice and followed the development of tumors over the course of several weeks. We found that the GFP and PID L107F cells quickly developed into tumors, reaching an average diameter of 2000 mm^3 by 3 weeks post-injection. In comparison, PID expressing cells resulted in much smaller tumors (average diameter of 1400 mm^3) at a considerably delayed rate (Fig. 5C). Finally, we found that the PID expressing tumors showed a reduced activity of Erk and Akt signaling pathways in comparison with the control cell lines derived tumors (Fig. 5D). These results indicate that suppression of Pak can at least partially inhibit the ability of ErbB2 to induce tumor formation in a xenograft model, consistent with the *in vitro* results obtained in our 3D cell culture system.

Discussion

Emerging evidence suggests that Pak1 plays an important role in human breast cancer (Dummler et al., 2009). For example, Pak1 expression levels are frequently elevated in breast cancer, often in association with amplification of the 11q13.5 chromosomal locus containing the Pak1 gene, and elevated expression of Pak1 is associated with tamoxifen-resistant disease (Rayala et al., 2006). In addition, transgenic expression of Pak1 in mouse mammary tissue is tumorigenic (Wang et al., 2005). However, the relationship of Pak1 to ErbB2 signaling, which is amplified in ~25% of human breast cancers, has not been previously examined. Here, we have shown that (i) ErbB2 expression correlates with Pak levels and enzymatic activity in ER-positive human breast cancer, (ii) that ErbB2 activates Rac and Pak in a 3D breast epithelial cell culture system, (iii) that loss of Rac or Pak activity blocks the morphologic effects of ErbB2 in these cells, accompanied by loss of Erk and Akt activation, (iv) that constitutive active versions of Rac or Pak recapitulate many of the features of ErbB2 signaling, and (v) that Pak activity is required for ErbB2 transformation in a xenograft model of breast cancer. These results show that Rac-Pak signaling is a key element in ErbB2 function in breast epithelial cells, and, for the first time, demonstrate that inhibiting Pak activity impedes breast tumor growth in animals.

In agreement with our results, Arteaga's group has also implicated the Rac1-Pak1 pathway in ErbB2 signaling in MCF-10A cells (Wang et al., 2006). This group found that TGFβ acts in concert with ErbB2 to stabilize an actin cytoskeletal complex containing, among other proteins, PI3K, Vav2, Rac1, and Pak1, resulting in prolonged activation of Rac1, enhanced cell invasiveness, Bad phosphorylation and enhanced cell survival. Our findings are also consistent with, but extend, recent discoveries from the Mattingly laboratory, which showed

that Pak1 plays an important role in a Ras-driven *in vitro* model for premalignant progression in mammary carcinogenesis (Li et al., 2008). In these experiments, Rac-Pak signaling was shown to affect acinar morphogenesis, invasiveness, and pericellular proteolysis in a series of Ras-transformed MCF-10A cells. However, Pak over- or under expression did not affect the phosphorylation of the Pak1 substrate LIM kinase or of its substrate cofilin, and effects on other Pak-regulated signaling molecules were not reported. Thus, the molecular events underlying these phenomena are unclear, and may not, in any case, be relevant to ErbB2-driven breast cancer models.

Pak activates a number of signaling pathways likely to be germane to ErbB2 signaling. Interestingly, Weigelt *et al.* have shown that ErbB2 oncogenic signaling in such cells depends on the PI3K/Akt pathway when the cells are grown in 2D conditions, but the Ras/Erk pathway when grown in 3D (Weigelt et al., 2009). It is well established that Paks play a role in the activation of Erk, most likely by phosphorylating c-Raf and Mek1 (Hofmann et al., 2004). Our results are consistent with this model, in that loss of Pak function by expression of dominant negatives or the PID, or by addition of a specific small molecule Pak inhibitor, all blocked morphologic transformation and Erk activation in response to ErbB2. In addition, treatment of 10A.ErbB2 cells with a Mek inhibitor had a similar effect, suggesting that Pak signaling to Erk was important for the effects of ErbB2 on acinar development. Loss of Pak also impeded Akt activation by ErbB2 (Fig. 4B), whereas overexpression of activated Pak1 increased it (Supplementary Fig. 4B). While the relationship of Pak to Akt signaling is less clear than for Erk, we have previously noted that in *Pak1*$^{-/-}$ cardiomyocyles, Akt is not responsive to a number of agonists such as IGF-1, and that Pak1 can phosphorylate Akt on S473 *in vitro* (Mao et al., 2008). Higuchu *et al.* have recently shown that Pak is required for Akt activation in COS1 cells, and suggested that Pak1 acts as a scaffold to link PDK1 to Akt (Higuchi et al., 2008). It is likely that all our inhibitors of Pak signaling (dominant negatives, the PID, and IPA-3) interfere not only with Pak kinase activity, but also with such scaffolding functions as well. For example, the small molecular Pak inhibitor IPA-3 works by an allosteric mechanism, altering Pak conformation and potentially blocking "opening" of the autoinhibited state (Deacon et al., 2008; Viaud & Peterson, 2009). BAD represents another potentially relevant Pak substrate, as Pak1 is known to phosphorylate this protein and loss of Pak blocks the pro-survival effects of ErbB2 during acinar development (Fig. 3A). Finally, it is interesting to note that nuclear Pak1 accumulation is associated with tamoxifen resistance in human breast cancer (Holm et al., 2006), and mutants of Pak1 that cannot localize to the nucleus fail to rescue the phenotype associated with Pak1 loss in zebrafish embryos (Lightcap et al., 2009). These results point to the possibility of critical nuclear substrates for Pak1, such as the estrogen receptor and perhaps other proteins that remain to be identified.

That Pak inhibition blocks Erk activation in ErbB2 transformed cells could have important therapeutic implications, as ErbB2-positive, ER-positive tumors have been reported to maintain activated Erk even when ErbB2 is blocked by inhibitory antibodies (Shou et al., 2004; Treeck et al., 2003). In this case, it is thought that estradiol signaling provides an ErbB2-independent input to the Erk pathway. Given that Pak inhibition blocks Erk activity in an ErbB2-positive, ER-negative (10A.ErbB2) as well as an ErbB2-positive, ER-positive

tumor cell line (MDA-MB-631/DYT2), Pak may represent a useful therapeutic target irrespective of ER status.

Recently, progress has been made on the development of specific Pak inhibitors (Deacon *et al.*, 2008; Maksimoska *et al.*, 2008; Porchia *et al.*, 2007; Viaud and Peterson, 2009). Here, we show for the first time that such small molecule inhibitors can block ErbB2 signaling in a 3D cell culture system. In addition, given the xenograft results, which used the PID as a Pak inhibitor *in vivo*, our results suggest that effective Pak inhibitors might be beneficial in ErbB2-driven breast cancer.

Materials and methods

Materials

Anti-ERK, -BAD, and all phospho-specific antibodies were purchased from Cell Signaling Technology. Monoclonal anti-ErbB2 was from Ventana Medical Systems, monoclonal anti-hemagglutinin (HA) (12CA5) was from BabCo, and anti-Ki-67 and anti-GST were from Santa Cruz. Reconstituted basement membrane (rBM; Matrigel) was purchased from BD Life Science, the Rac inhibitor NSC23766 from Calbiochem, and Oregon Green phalloidin from Molecular Probes.

Tissue microarray (TMA)

Breast cancer specimens of at least 100 mg were obtained from the tumor core at the time of surgery from each patient per an Institutional Review Board approved protocol. The specimens were verified as invasive mammary carcinomas by a pathologist. The specimens were then immediately frozen in liquid nitrogen and stored at −80°C for subsequent assay preparations. The archived H&E slides used for diagnosis were reviewed by the pathologist on the team for confirmation of diagnosis and selection of appropriate paraffin-embedded tissue blocks for the construction of TMAs. Slides with appropriate tissue of interest were selected and mapped to define representative areas for construction of the TMA blocks using a 1.5 mm punch size.

Immunohistochemistry

5 μm thick sections were cut, warmed to 60°C, de-paraffinized in xylene, and then rehydrated with graded ethanol. Antigen exposure took place for 20 minutes in heated antigen retrieval solution and then the endogenous peroxide activity was inactivated by treating with 0.3% H_2O_2 in methanol. The sections were blocked for 20 min in normal goat serum in PBS, and incubated with primary antibodies against ErbB2 or pPak, for 1h using an automated stainer. Samples were rinsed 5 times in washing buffer, and incubated in secondary antibody for 30 min. Samples were rinsed 3 times in wash buffer, and then incubated in horseradish peroxidase label (BioGenex) for 15 min. Samples were rinsed 3 times in wash buffer and then incubated in diaminobenzidine for 5 min. Samples were rinsed 3 times in wash buffer and counterstained in hematoxylin for 2 min. A semiautomated quantitative image analysis system, ACIS II (Chromavision), was used to evaluate the same TMA slides. Proprietary software is used to detect the brown stain intensity of the chromogen used for the immunohistochemical analysis and compares this value to blue

counterstain used as background. Theoretical intensity levels range from 0 to 255 chromogen intensity units. For graphics purposes, P-Pak intensity scores of 0–60, 61–120, 121–180, and 181–244 were termed groups 1, 2, 3, and 4 respectively.

Cell lines and 3D cell culture

10A.ErbB2 cells (MCF-10A cells expressing a chimeric form of ErbB2) (Muthuswamy et al., 2001) and 10A.ErbB2/ErbB1 cells (MCF-10A cells expressing a chimeric form of ErbB2 and ErbB1) (Muthuswamy et al., 2001) (were maintained in DMEM/F12 (Gibco BRL) supplemented with 5% donor horse serum, 20 ng/ml EGF (Harlan Bioproducts), 10 μg/ml insulin (Sigma), 1 ng/ml cholera toxin (Sigma), 100 μg/ml hydrocortisone (Sigma), 50 U/ml penicillin and 50 μg/ml streptomycin. For 3D cultures, the ~5,000 cells were plated atop rBM in 8-well slide chambers as described (Muthuswamy et al., 2001). To activate chimeric ErbB proteins, 1 μM AP1510 was added to the growth medium. BT-474, BT-20, SKBR-3, and MDA-MB-361/DYT2 were grown in RPMI, 10% fetal bovine serum.

Viruses

Tetracycline-regulated recombinant adeno viruses bearing Myc-Rac1 G12V, Myc-Rac1 T17N, HA-Pak1 L107F and HA-Pak1 K299 were obtained from Dan Kalman (Srinivasan et al., 2003). Similar adenoviruses, bearing the Pak inhibitor domain (PID) or an inactive control (PID L107F), were constructed using the pAd-lox system (Hardy et al., 1997). For adenoviral transduction, 10A.ErbB2 cells were plated at 3×10^5 cells per 10-cm-diameter dish, then doubly infected with high-titer adenoviruses bearing the transgene of interest and the tetracycline transactivator, respectively. Lysates were screened by anti-GST or anti-myc immunoblots to measure expression.

Retroviruses bearing the PID or PID L107F were constructed using pBMN-I-GFP (a gift from Garry Nolan, Stanford University). Recombinant viruses were generated using the Phoenix amphotropic packaging system (Kinsella & Nolan, 1996).

Immunoblotting, and In-Cell Westerns

Cells were lysed in a buffer containing 50 mM Tris-HCl, pH 8.0, 137 mM NaCl, 10% glycerol, 1% NP-40, 50 mM NaF, 10 mM β-glycerol-phosphate, 2 mM sodium orthovanadate, 1 mM phenylmethylsulfonyl fluoride, and 10 μg/ml aprotinin. Immunoblots (on Immobilon-P membranes (Millipore)) were blocked with 5% BSA or non-fat dry milk in 10 mM Tris-HCl, pH 7.4, 150 mM NaCl, and 0.05% Tween-20. After incubation with appropriate primary and secondary antibodies, blots were visualized using enhanced chemiluminescence reagents (ECL; Amersham Biosciences). Quantification was carried out using NIH ImageJ Software Version 1.40; data are expressed as relative units of phosphorylated protein per total protein for each band. Anti-Pak1 and anti-Rac1 antisera were used at 1/1000 for immunoblotting. All other antibodies were used at concentrations as recommended by the supplier.

For in-cell westerns, cells were fixed in 4% methanol-free formaldehyde in phosphate-buffered saline (PBS), rinsed with PBS, blocked with 5% non-immune rabbit or mouse serum in PBS/0.1% Triton X-100 for 1 hr, and incubated with primary antibodies for two hr

at 37°C. The cells were then rinsed three times in PBS for 5 minutes each, then Incubated in fluorochrome-conjugated secondary antibody diluted 1:500 (Alexa Fluor® 680) or 1:800 (IRDye 800 CW) in PBS/0.1% Triton for one hour at room temperature in the dark. The cells were then rinsed three times in PBS for 5 minutes each, and scanned using a Li-Cor Odyssey device.

GST-PBD pull down

Glutathione-Sepharose beads carrying GST fused to the PBD of Pak1 were used to immunoprecipitate Rac from cell treated with 1 μM AP1510 for 20 min. Lysates were incubated with GST-PBD beads for 1 h at 4°C with continuous rotation. Beads were then washed several times, and the bound material was eluted using sample buffer for 5 min at 90°C. The eluate was resolved on 12% SDS-PAGE gels and analyzed by immunoblot.

Immunofluorescence analysis

The acinar structures were fixed in 4% paraformaldehyde at room temperature for 15 min, and processed as described (Muthuswamy et al., 2001). Confocal analyses were performed with a Nikon TE2000 confocal microscopy system.

Xenografts

Four- to 6-week-old inbred C.B17/Icr-SCID mice were obtained from the Fox Chase Cancer Center Laboratory Animal Facility. MDA-361/DYT2 cells expressing GFP, PID or PID L107F (5×10^6 in 0.3 ml of rBM) were injected subcutaneously into the abdomen of each mouse. The mice were observed and weighted and their tumors were measured with calipers every 3 days. All studies described in this article were done under approved protocols following Fox Chase Cancer Center Institutional Animal Care and Use Committee guidelines. Mice were euthanized when tumor volumes exceeded 10% of the animal's body weight or at 30 days post-initiation of the experiment, whichever occurred first.

Statistics

Relationships between the expression levels of different markers evaluated in the TMA were explored using Spearman rank correlation. For the xenograft studies, treatment cohorts were analyzed by one-way ANOVA using the GraphPad InStat 3 software package (GraphPad Software).

Supplementary Material

Refer to Web version on PubMed Central for supplementary material.

Acknowledgments

Abbreviations

|	
CA	Constitutive active
DN	Dominant negative
ER	estrogen receptor
GST	glutathione-S-transferase
PBD	p21-binding domain
Pak	p21-activated kinase
IHC	immunohistochemistry
PBS	phosphate-buffered saline
PID	Pak inhibitor domain
RTK	Receptor protein tyrosine kinase
rBM	reconstituted basement membrane
3D	three-dimensional
TMA	Tissue microarray

References

Amundadottir LT, Leder P. Oncogene. 1998; 16:737–746. [PubMed: 9488037]

Deacon SW, Beeser A, Fukui JA, Rennefahrt UE, Myers C, Chernoff J, Peterson JR. Chem Biol. 2008; 15:322–331. [PubMed: 18420139]

Dummler B, Ohshiro K, Kumar R, Field J. Cancer Metastasis Rev. 2009; 28:51–63. [PubMed: 19165420]

Gao Y, Dickerson JB, Guo F, Zheng J, Zheng Y. Proc Natl Acad Sci U S A. 2004; 101:7618–7623. [PubMed: 15128949]

Hardy S, Kitamura M, Harris-Stansil T, Dai Y, Phipps ML. J Virol. 1997; 71:1842–1849. [PubMed: 9032314]

Higuchi M, Onishi1 K, Kikuchii C, Gotoh Y. Nat Cell Biol. 2008; 10:1356–64. [PubMed: 18931661]

Hofmann C, Shepelev M, Chernoff J. J Cell Sci. 2004; 117:4343–54. [PubMed: 15331659]

Holm C, Rayala S, Jirstrom K, Stal O, Kumar R, Landberg G. J Natl Cancer Inst. 2006; 98:671–680. [PubMed: 16705121]

Hynes NE, MacDonald G. Curr Opin Cell Biol. 2009; 21:177–184. [PubMed: 19208461]

Karunagaran D, Tzahar E, Beerli RR, Chen X, Graus-Porta D, Ratzkin BJ, Seger R, Hynes NE, Yarden Y. EMBO J. 1996; 15:254–264. [PubMed: 8617201]

Kinsella TM, Nolan GP. Hum Gene Ther. 1996; 7:1405–1413. [PubMed: 8844199]

Li Q, Mullins SR, Sloane BF, Mattingly RR. Neoplasia. 2008; 10:314–329. [PubMed: 18392133]

Lightcap CM, Kari G, Arias-Romero LE, Chernoff J, Rodeck U, Williams JC. PLoS One. 2009; 4:e6025. [PubMed: 19557173]

Mao K, Kobayashi S, Jaffer ZM, Huang Y, Volden P, Chernoff J, Liang Q. J Mol Cell Cardiol. 2008; 44:429–434. [PubMed: 18054038]

Muthuswamy SK, Li D, Lelievre S, Bissell MJ, Brugge JS. Nat Cell Biol. 2001; 3:785–792. [PubMed: 11533657]

Rayala SK, Molli PR, Kumar R. Cancer Res. 2006; 66:5985–5988. [PubMed: 16778166]

Author Manuscript Author Manuscript Author Manuscript Author Manuscript

Schnelzer A, Prechtel D, Knaus U, Dehne K, Gerhard M, Graeff H, Harbeck N, Schmitt M, Lengyel E. Oncogene. 2000; 19:3013–3020. [PubMed: 10871853]

Shou J, Massarweh S, Osborne CK, Wakeling AE, Ali S, Weiss H, Schiff R. J Natl Cancer Inst. 2004; 96:926–935. [PubMed: 15199112]

Soule HD, Maloney TM, Wolman SR, Peterson WDJ, Brenz R, McGrath CM, Russo J, Pauley RJ, Jones RF, Brooks SC. Cancer Res. 1990; 50:6075–6086. [PubMed: 1975513]

Srinivasan S, Wang F, Glavas S, Ott A, Hofmann F, Aktories K, Kalman D, Bourne HR. J Cell Biol. 2003; 160:3375–3385.

Treeck O, Diedrich K, Ortmann O. Eur J Cancer. 2003; 39:1302–1309. [PubMed: 12763221]

Viaud J, Peterson JR. Mol Cancer Ther. 2009; 8:2559–2565. [PubMed: 19723886]

Wang SE, Shin I, Wu FY, Friedman DB, Arteaga CL. Cancer Res. 2006; 66:9591–9600. [PubMed: 17018616]

Wang RA, Zhang H, Balasenthil S, Medina D, Kumar R. Oncogene. 2005; 25:2931–2936. [PubMed: 16331248]

Weigelt B, Lo AT, Park CC, Gray JW, Bissell MJ. Breast Cancer Res Treat. 2009; 122:35–43. [PubMed: 19701706]

Zhan L, Xiang B, Muthuswamy SK. Cancer Res. 2006; 66:5201–5208. [PubMed: 16707444]
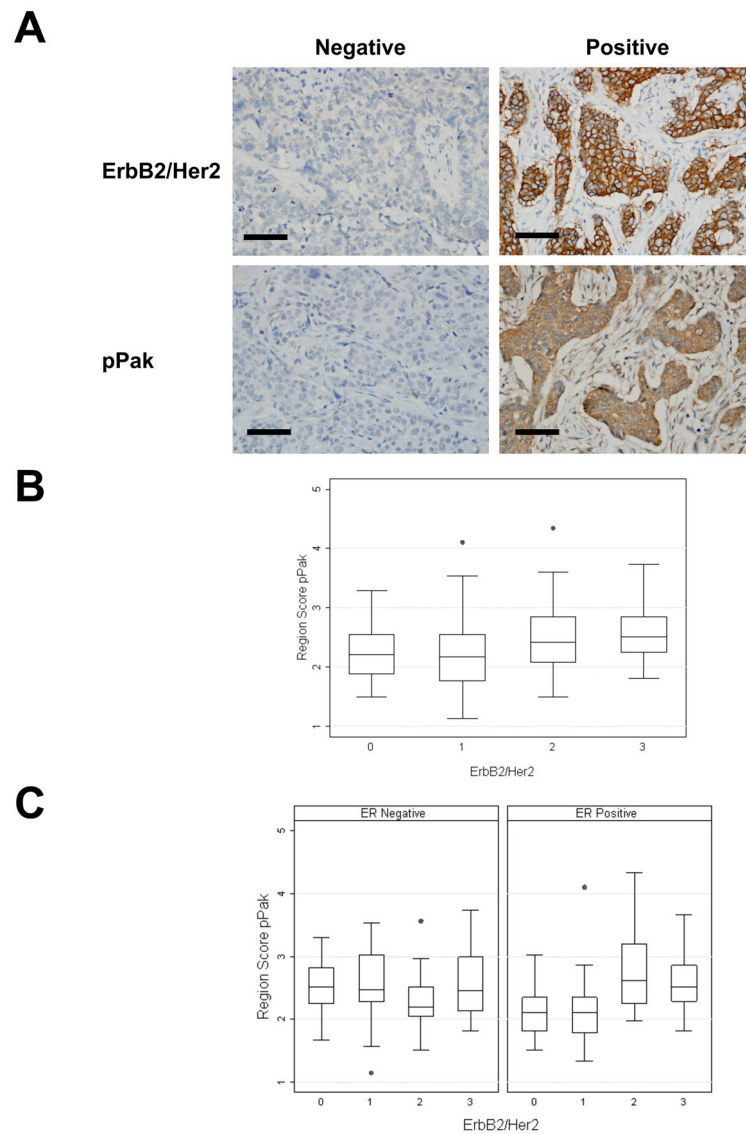
Figure 1. Correlation of immunohistochemical staining of ErbB2 and phospho-Pak in human breast cancer

A, Representative example of human breast cancer specimens from TMA that stained positive or negative for ErbB2. Matching specimens from the same patient are shown for phospho-Pak. Size bar = 10 μm. B, TMA-IHC analysis. Correlation of ErbB2 expression with phospho-Pak, the graphic represent the integrated optical density (Region Score) of immunohistochemical staining intensity (r=0.2938, p<0.0001). X axis = ErbB2 staining score (0–3); y axis = P-Pak intensity score (0–4). C, Correlation of ErbB2 expression with phospho-Pak in ER negative and positive samples, the graphics represent the integrated optical density (Region Score) of immunohistochemical staining intensity (r=−0.0428, p=0.7327 and r=0.4342, p<0.0001 respectively)
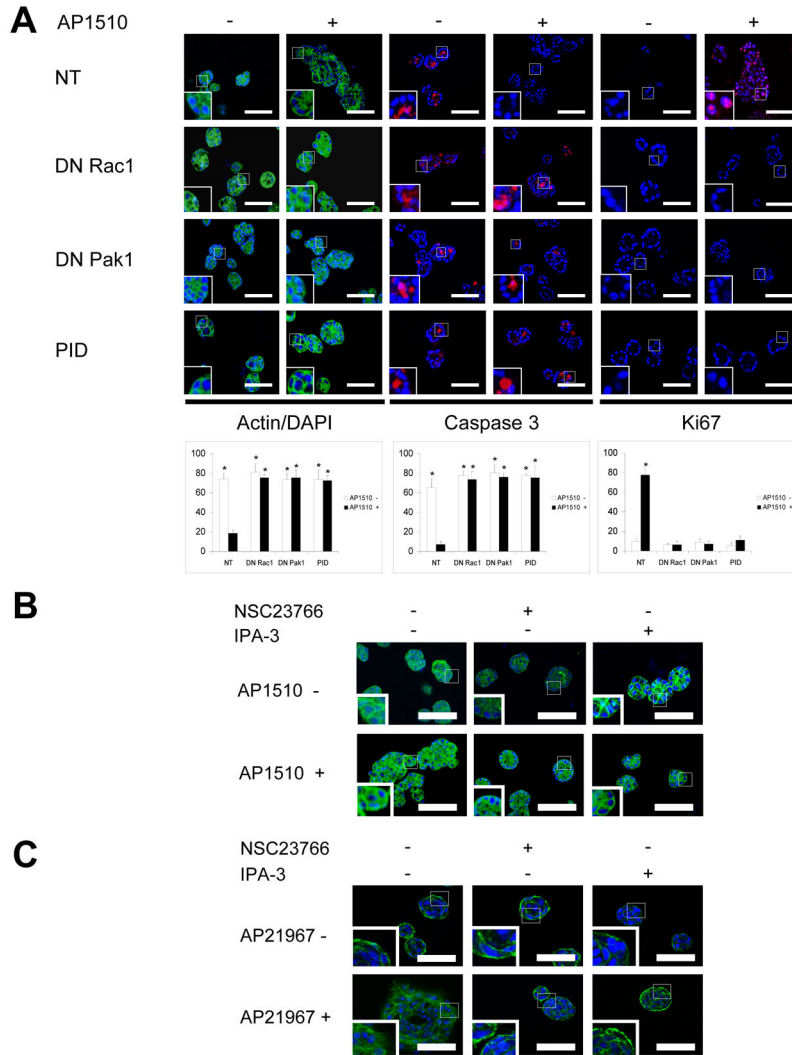
Figure 2. Pak is required for ErbB2-mediated transformation of MCF-10A cells
A, 10A.ErbB2 cells were transduced with empty adenovirus or adenoviruses encoding DN
Rac1 (Rac1 T17N), DN Pak1 (Pak1 K299R), or the PID, plus an adenovirus encoding a
tetracycline transactivator, and plated atop reconstituted basement membrane. Cells were
stimulated with vehicle or 1 μM AP1510 on day 3 and fixed on day 12 and stained with
Oregon green-phalloidin, Ki-67, or anti-cleaved caspase-3. Insets show higher magnification
images. Graphics represent the percentage of unilamellar acini, Ki-67-positive, and anti-
cleaved caspase-3-positive acini were scored based on assessment of 50 to 60 acini per well,
counting cells in four planes of each acinus. *$p<0.05$ Size bar = 50 μm. B, 10A.ErbB2 cells
plated atop reconstituted basement membrane were treated with vehicle, 20 μmol/L
NSC23766, or 10 μmol/L IPA-3, plus 1 μmol/L AP1510, on day 3 as indicated, and fixed on
day 12. Medium was replaced (with Rac and Pak inhibitors and AP1510) every 3 days. Cells
were stained with Oregon green-phalloidin and DAPI. C, 10A.ErbB2/ErbB1 cells plated
atop reconstituted basement membrane were treated with vehicle, 20 μmol/L NSC23766, or
10 μmol/L IPA-3, plus 1 μmol/L AP21967, on day 3 as indicated, and fixed on day 12. Cells
were stained with Oregon green-phalloidin and DAPI.
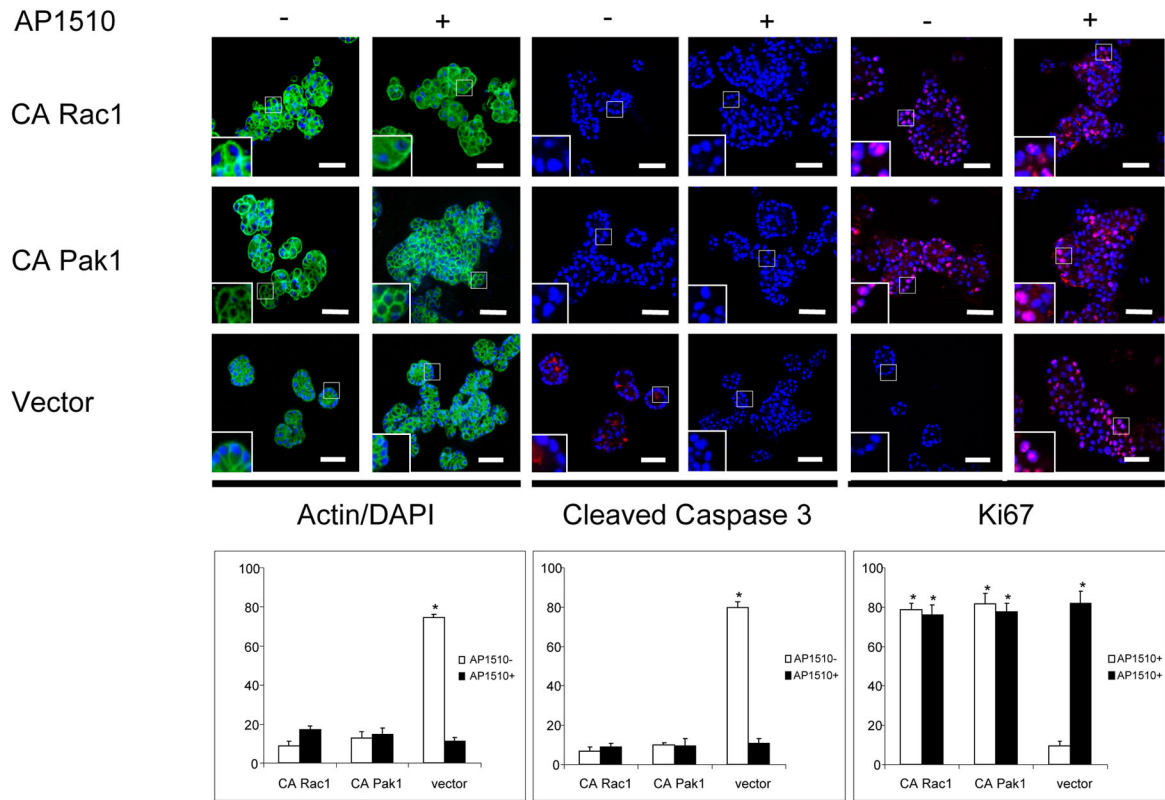
Figure 3. Activated Pak bypasses requirement of ErbB2 activity for transformation

10A.ErbB2 cells were transduced with adenoviruses encoding constitutively active (CA) forms of Rac1 (Rac1 G12V) or Pak1 (Pak1 L107F), or a control adenovirus, plus an adenovirus encoding a tetracycline transactivator, and plated atop reconstituted basement membrane. Cells were stimulated with vehicle or AP1510 on day 3 and fixed on day 12 and processed as before. Insets show higher magnification images. Size bar = 50 μm. Graphics represent the percentage of unilamellar acini, Ki-67-positive, and anti-cleaved caspase-3-positive acini were scored based on assessment of 50 to 60 acini per well. *$p<0.05$.
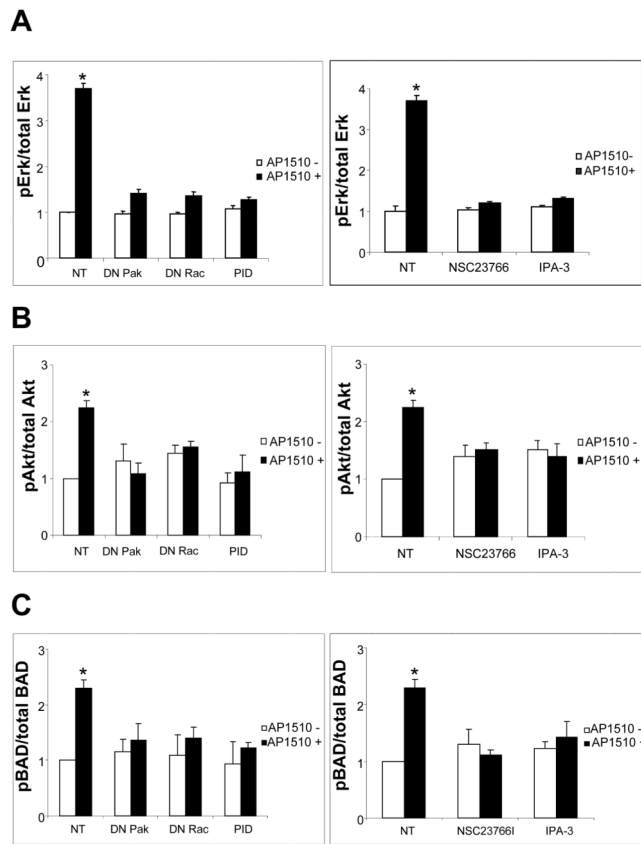
Figure 4. Pak inhibition down-regulates proliferation signaling pathways in MCF-10A cells
10A.ErbB2 cells were transduced with adenoviruses encoding DN forms of Rac or Pak, or treated with their specific small-molecule inhibitors and plated atop reconstituted basement membrane. Cells were stimulated with vehicle or AP1510 on day 3 and fixed on day 12. The activity of ERK (A), Akt (B), and BAD (C) was assessed by in-cell Western using phospho specific antibodies. *p<0.05

A

B

C

D
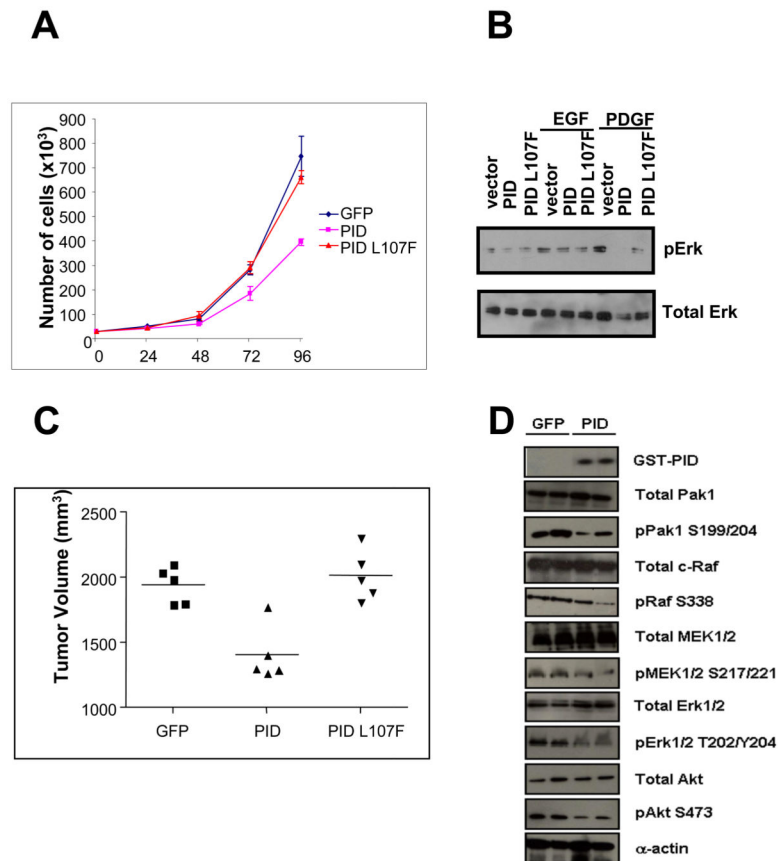
Figure 5. Downregulation of Pak inhibits the tumorigenicity of MDA-MB-631/DYT2 cells *in vivo*
A, 3×10^4 MDA-MB-631/DYT2 cells stably expressing GFP, PID or PID L107F were
plated in triplicate into 12-well plates. Cells were harvested and counted at 0, 24, 48, 72 and
96 h. The data are representative of three independent experiments. *Points,* mean; *bars,* SD.
B, Immunoblot analysis of ERK activation in MDA-MB-631/DYT2 cells expressing GFP,
PID or PID L107F. C, Tumor size distribution in SCID mice. Tumor formation was assessed
by injecting 5×10^5 MDA-MB-631/DYT2 cells infected with either empty virus (GFP), PID
or PID L107F into the flanks of the mice. Five mice were used in total for each group. The
size of tumors was measured three weeks after injection. Horizontal lines, average tumor
diameters. D, Western analysis shows expression and activation levels of the indicated
proteins in primary tumor lysates and quantification of relative difference in activation
between GFP and PID expressing tumors.